

Modeling Air Blast on Thin-shell Structures with Zapotec

Greg C. Bessette, Courtenay T. Vaughan, Raymond L. Bell, and Stephen W. Attaway
Sandia National Laboratories
P.O. Box 5800
Albuquerque, NM 87185-0820

A new capability for modeling thin-shell structures within the coupled Euler-Lagrange code, Zapotec, is under development. The new algorithm creates an artificial material interface for the Eulerian portion of the problem by expanding a Lagrangian shell element such that it has an effective thickness that spans one or more Eulerian cells. The algorithm implementation is discussed along with several examples involving blast loading on plates.

INTRODUCTION

Modeling air blast on thin-shell structures poses a significant challenge for Eulerian hydrocodes such as CTH. The fine mesh resolution required to adequately model the thin-shell response is difficult to achieve for 3D applications and is an overriding concern when the shell thickness is smaller than the length scale associated with other materials in the problem. Another issue is modeling the long-term transient response of the structure itself. For blast applications, the duration of the blast loading is often orders of magnitude less than the response time associated with the structure, making it costly to conduct a pure Eulerian calculation to assess the late-time structural response.

In this paper, we describe the development of a shell reconstruction algorithm implemented into the Zapotec code specifically for modeling blast applications involving thin-shell structures. Zapotec is a coupled Euler-Lagrange code that links two production codes, CTH and Pronto3D. Zapotec was originally developed for modeling penetration applications, but recent development has focused on blast/structure interaction problems. The shell reconstruction algorithm recently implemented into Zapotec is designed to accommodate Lagrangian thin-shell structures discretized using 4-node quadrilateral shell elements. The algorithm is oriented towards applications where the shell thickness is much smaller than the corresponding CTH cell size.

In the remainder of this paper, we provide a general description of the Zapotec coupling algorithm as well as a description of the shell reconstruction algorithm and its implementation. We then demonstrate the utility of the algorithm for several example problems.

ZAPOTEC COUPLING ALGORITHM

Zapotec is a coupled Euler-Lagrange code that links the CTH and Pronto3D codes [1,2]. CTH, an Eulerian shock physics code, performs the Eulerian portion of the calculation, while Pronto3D, an explicit finite element code, performs the Lagrangian portion. The two codes are run concurrently with the appropriate portions of a problem solved on their respective computational domains. Zapotec handles the coupling between the two computational domains. Both CTH and Pronto3D are well documented (e.g., see [3,4,5,6]) and the remaining discussion will focus on the Zapotec coupling algorithm.

Zapotec controls both the time synchronization between CTH and Pronto3D as well as the interaction between materials on their respective computational domains. At a given time t_n , Zapotec performs the coupled treatment between the Eulerian and Lagrangian materials in the problem. Once this treatment is complete, both CTH and Pronto3D are run independently over the next Zapotec time step. In general, the Pronto3D stable time step will be smaller than that for CTH. When this occurs, Zapotec allows subcycling of the Pronto3D code for computational efficiency and accuracy. Zapotec ensures the two codes reach the same time t_{n+1} at the end of the Zapotec time step.

An outline of the Zapotec coupled treatment is provided in Fig. 1. The coupled treatment at time t_n involves getting data from CTH and Pronto3D, working on the data, then passing the updated data back to the two codes. Zapotec first operates on the CTH data, a process termed material insertion. This involves mapping the current configuration (and state) of a Lagrangian body onto the fixed Eulerian mesh. The insertion algorithm determines what portions of a Lagrangian body are overlapping the CTH mesh. Material state data from the overlapping Lagrangian body are

then mapped into cells in the CTH mesh. Mapped data include the mass, momentum, stress, sound speed, and internal energy. In general, a CTH cell will be overlapped by several Lagrangian elements. When this occurs, the mapped Lagrangian quantities for each element are weighted by their volume overlap. The exception is the deviatoric stress, which is mass-weighted. The weighted quantities are accumulated for all elements overlapping a cell, after which the intrinsic value is recovered for insertion. The inserted data are then passed back to CTH as a mesh update.

- (1) Remove pre-existing Lagrangian material from the CTH mesh
- (2) Get updated Lagrangian data
- (3) Insert Lagrangian material into the CTH mesh
 - (a) Compute volume overlaps
 - (b) Map Lagrangian data – mass, momentum, stress, sound speed, internal energy
 - (c) Pass updated mesh data back to CTH
- (4) Compute external forces on Lagrangian surface
 - (a) Determine surface overlaps
 - (b) Compute surface tractions based on Eulerian stress state
 - (c) Compute normal force on element surface (element-centered force)
 - (d) If friction, compute tangential force
 - (e) Distribute forces to nodes and pass data back to Pronto3D
- (5) Execute Pronto3D and CTH

Figure 1. Summary of the Zapotec Coupling Algorithm

Once the material insertion is complete, the external loading on a Lagrangian material surface is determined from the stress state in the neighboring Eulerian mesh. Since the Lagrangian material surface is uniquely defined, it is straightforward to determine the external forces on a Lagrangian surface element from the traction vector, the element surface normal, and element area. Zapotec can also evaluate frictional contact based on a Coulomb friction model, a useful option for penetration applications. After the applied loads are determined on each Lagrangian surface element, the element-centered forces are distributed to the nodes and passed back to Pronto3D as a set of external nodal forces. Once the coupled treatment is complete, both CTH and Pronto3D are run independently over the next time step with their updated data.

SHELL RECONSTRUCTION ALGORITHM

The shell reconstruction algorithm is designed to accommodate thin-shell structures, where the shell thickness is significantly smaller than the corresponding CTH cell width. In the present context, we are interested in the treatment of Lagrangian thin-shell structures discretized using 4-node quadrilateral shell elements. Specifically, we only consider elements supported by Pronto3D, which include shells based on the Belytschko-Lin-Tsay and Key-Hoff formulations (see [6] for details). The shell reconstruction algorithm creates an artificial material interface for CTH by expanding the shell element thickness so that it has an effective thickness that spans one or more cells. The expanded shell now has significant volume, which is inserted into the CTH mesh as part of the Zapotec coupling algorithm. The external loading on the outer surface of the expanded shell is then assessed, with the loads passed back to Pronto3D as a set of external nodal forces. The following procedure outlines the shell reconstruction algorithm for a single shell element:

Step 1: Determine the effective shell thickness

The effective shell thickness $t_{\text{eff,shell}}$ is based on the minimum effective cell width for all cells in the mesh, and is computed as

$$t_{\text{eff,shell}} = (\text{scale}) \min \{L_e\}, \text{ where } L_e = \sqrt{w_x^2 + w_y^2 + w_z^2} \quad (1)$$

L_e is the diagonal length of a CTH cell, w_x , w_y , and w_z are the cell widths along the x-, y-, and z-coordinate axes. The user has the option to modify the effective shell thickness using a prescribed scaling factor, denoted by the term scale above.

Step 2: Create the expanded shell

This procedure is illustrated in Fig. 2 using a simple 2D example. In this step, the thin shell element is essentially transformed into a hexahedral element. In order to complete the transformation process, it is necessary to determine a direction for extending the shell thickness. This direction is based upon the average surface normal \mathbf{n} , which is computed as

$$\begin{aligned} \mathbf{r}' &= (\mathbf{x}_2 - \mathbf{x}_1) + (\mathbf{x}_3 - \mathbf{x}_4) \\ \mathbf{s}' &= (\mathbf{x}_4 - \mathbf{x}_1) + (\mathbf{x}_3 - \mathbf{x}_2) \\ \mathbf{r} &= \mathbf{r}' / |\mathbf{r}'| \quad \mathbf{s} = \mathbf{s}' / |\mathbf{s}'| \\ \mathbf{n} &= \mathbf{r} \times \mathbf{s} \end{aligned} \quad (2)$$

where \mathbf{x}_i are the nodal coordinates for the four vertex nodes, \mathbf{r} and \mathbf{s} are directional vectors defining the shell surface orientation. Once the average surface normal is determined, it is a straightforward procedure to determine the corners of the expanded shell. In the algorithm, new nodes are created at the corners of the expanded shell, which in turn, are used to define the top and bottom surfaces of the expanded shell. It is assumed that the outward pointing average surface normal defines the top surface of the expanded shell.

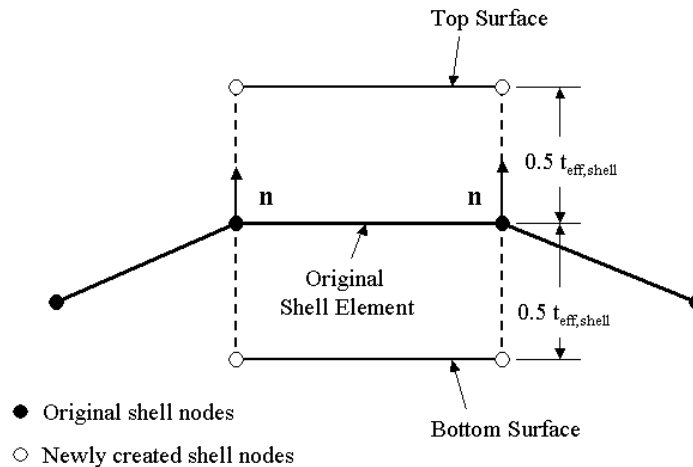


Figure 2. Illustration of Shell Reconstruction Algorithm

Step 3: Insert expanded shell into CTH mesh

The procedure for material insertion (Step (3) in Fig. 1) follows that used for other element types (e.g., the constant strain hexahedral and tetrahedral elements supported by Pronto3D) with some exceptions. First, shell elements have stresses computed at each of the through-thickness integration points. The insertion algorithm requires a single stress state. By default, the stresses at the integration points are averaged with the averaged stress state used by the material insertion algorithm. However, the user has the option to use the stress state at a particular integration point. Also, the material density, which is used to compute the inserted element mass, is modified prior to insertion. The true material density is scaled by the ratio of true shell to expanded shell volume in order to conserve the mass and momentum of the inserted material.

Step 4: Assess loading on the expanded shell surface

The loading on the exterior surface of the expanded shell is assessed in the manner described in step (4) of Fig. 1. The applied nodal forces are mapped from the surface nodes of the expanded shell onto the nodes of the original shell element. The mapped forces are then returned to Pronto3D as a set of external nodal forces. For thin-shell structures, there is the potential for interaction on both sides of the shell element within a CTH cell. This is accommodated in the problem setup, where the user has flexibility in defining the geometry of the expanded shell as well as defining the surface(s) (e.g., top, bottom, or both) that can interact with Eulerian materials.

Remark 1: Zapotec makes no attempt to check for overlapping expanded shell elements. This can potentially lead to errors when inserting materials with highly curved geometries or structures having irregular sections (e.g., T-sections). To illustrate this problem, consider the curved structure shown in Fig. 3. Expanded shell elements will overlap on the inside of the curved structure. Conversely, there will be gaps in the material insertion on the outside of the circular structure. Mass and momentum will be conserved; however, the distribution of mass and momentum will not be correct. This should not pose a significant problem for applications involving simple structures where the “action” takes place on one side (e.g., consider blast loading on a flat plate), but may pose problems when the loading occurs on both sides of the structure.

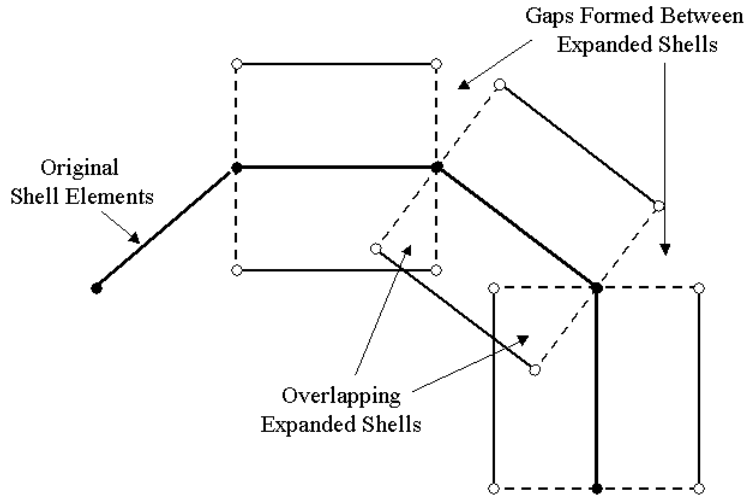


Figure 3. Potential Problems Encountered with Curved Structures

Remark 2: Zapotec makes no attempt to check for overlaps between expanded shell elements and other materials in the problem. For example, consider the joint between a thin-shell structure and a solid body composed of hexahedral elements (see Fig. 4), where both materials are defined as Lagrangian. If the shell structure deforms and starts to collapse onto the solid body, it is possible for expanded shell elements to overlap portions of the solid body. This can lead to over-filled cells in the vicinity of the joint, with a subsequent over-compression of materials as Zapotec attempts to insert both Lagrangian materials into an Eulerian cell containing air. There is no automated procedure for avoiding this problem and the user must exercise care with interpretation of results when this situation arises.

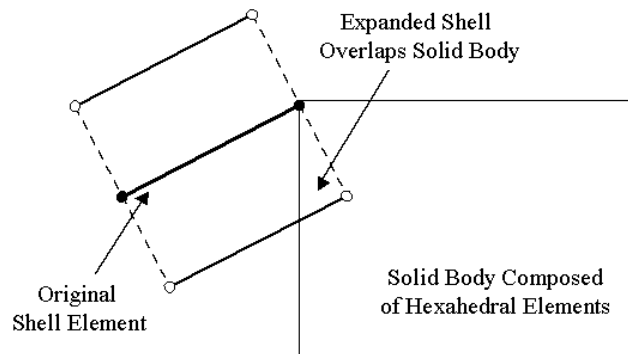


Figure 4. Illustration of Expanded Shell Overlapping a Solid Body

EXPLOSIVELY-DRIVEN PLATE

A series of demonstration problems have been analyzed to test the algorithm. The first involves an explosively-driven plate as described in [7]. Lee, et al. evaluated various detonation product equations of state (EOS) by measuring the velocity of a thin flat plate accelerated by an explosive. The explosive was detonated using an electronically-driven flyer plate, resulting in a planar detonation front in the explosive that induced an essentially

uniform loading across the plate. Comparisons were then made with high-resolution hydrocode calculations to assess various EOS implementations. Here, we will model one of these experiments (No. 9634) with Zapotec. In this experiment, a 19.95-mm-thick sample of LX-14 explosive is used to accelerate a 0.526-mm-thick copper plate. A Fabry-Perot velocimeter was used in the experiments to measure the particle velocity at the back surface of the copper plate. Comparisons will be drawn with the measured plate velocity.

The initial Zapotec problem setup is illustrated in Fig. 5. For the Zapotec analysis, the explosive is modeled as an Eulerian material, while the copper plate is considered Lagrangian. The CTH mesh encompasses the explosive and inserted plate as depicted in Fig. 5, with the surrounding region composed of void. The CTH mesh extends beyond the initial material configuration along the axial direction to allow room for the expanding detonation products and resulting plate motion. Outflow boundary conditions were assumed along the axial extents of the CTH mesh, with non-reflecting boundary conditions assumed along the lateral extents to model the plane strain condition induced in the experimental setup. The plate was modeled using a uniform mesh of Key-Hoff shell elements having a specified thickness and width of 0.526 and 0.16 mm, respectively. Symmetry and no rotation boundary conditions were applied to the edges of the finite element mesh to emulate plane strain conditions in the Lagrangian domain. The CTH material library Jones-Wilkins-Lee (JWL) EOS for LX-14-0 was used to model the hydrodynamic response of the explosive. The explosive was detonated simultaneously along a plane located at the x-axis origin. The response of the copper plate was modeled with the Johnson-Cook constitutive model using material data for OFHC copper as described in [8].

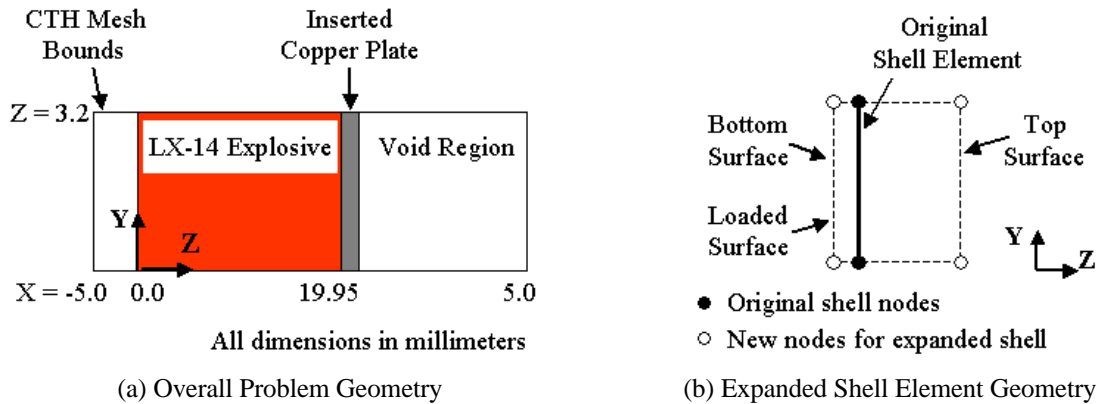


Figure 5. Zapotec Problem Setup

The user has the option to specify the shell expansion direction(s) during problem setup. For this problem, it is necessary to prescribe different expansion distances along the top and bottom surfaces of the shell mesh. Shell elements are expanded along the bottom direction (i.e., on the side contacting the explosive) to half of the plate thickness so that their expanded thickness coincides with their true location at the explosive/plate interface. Shell elements are expanded along the top direction to cover one or more CTH cells in the adjacent void space. By default, the shell reconstruction algorithm generates shell surfaces for the force application step. For this problem, it is desired to apply the external forces only along the bottom surface of the plate as shown in Fig. 5. This is done to reduce the cost of the surface overlap calculation noted in step (4) of Fig. 1.

Comparisons of the calculated nodal velocity at the plate centerline with the experimental results are provided in Fig. 6. Zapotec results are presented for two cases that will serve to investigate the influence of CTH mesh resolution on the calculated velocity. For each case a uniform CTH mesh was specified, having a cell size of either 0.8 or 0.2 mm. The cell size for the coarser mesh is greater than the plate thickness, while the finer mesh allows at least two cells to cover the true plate thickness. For both cases, a prescribed scale factor of two was applied for determination of the effective shell thickness along the top direction (i.e., scale = 2.0 in Eq. (1)). The results from an equivalent 1D rectangular ($\Delta x = 0.02$ mm) and a fully 3D CTH calculation ($\Delta x = 0.2$ mm) are provided for comparison.

The experimental results in Fig. 6 indicate a ramping up of the back surface velocity. This ramping correlates with the interaction of the incident blast wave with the plate and subsequent reflection of the transmitted wave off its free

surface. Each wave transit allows for an increase in the plate acceleration. Over time, the back surface plate velocity asymptotes to a measured value of 4.350 km/sec. The CTH-1DR calculation compares well with the experimental results, capturing the features of the velocity ramping at the rear surface of the plate. The CTH-3D calculation does not capture the velocity ramping (likely due to a lack of adequate mesh resolution), but does obtain an asymptotic velocity that compares well with the experimental data. The velocity ramping was not captured in either Zapotec calculation, with the asymptotic velocity noticeably over-predicted with the coarser CTH mesh and only a slight over-prediction for the finer mesh calculation. Numeric values for the calculated asymptotic velocities are provided in Table 1.

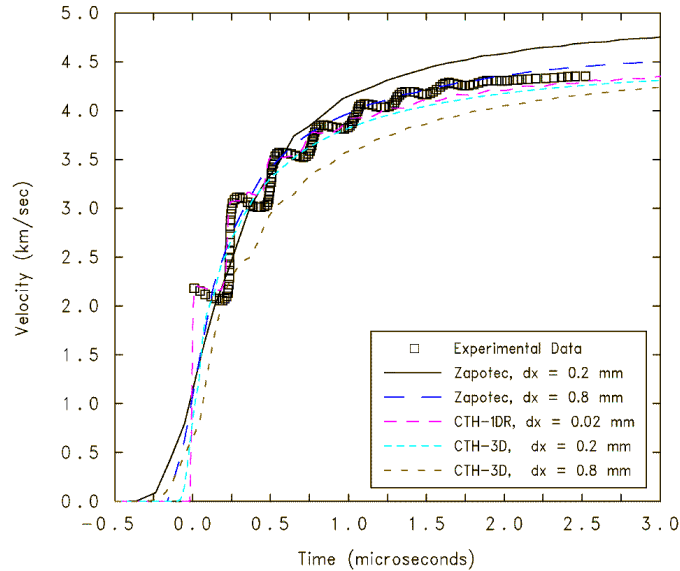


Figure 6. Comparison of Plate Velocities

Table 1. Comparison of Calculated Asymptotic Plate Velocity

Calculation	CTH Mesh Resolution (mm)	Calculated Plate Velocity (km/sec) as a Function of Effective Shell Thickness Scale Factor (Scale)		
		1.0	2.0	3.0
CTH-1DR	0.02	n/a	4.390	n/a
CTH-3D	0.20	n/a	4.356	n/a
CTH-3D	0.80	n/a	4.305	n/a
Zapotec	0.20	4.544	4.551	4.566
Zapotec	0.80	4.852	4.808	4.785

The shell element formulation assumes plane stress conditions along the thickness direction (i.e., $\sigma_{zz} = 0$ for this problem). As a result, the shock transit through the shell element is not captured and there is no mechanism for a velocity gradient along the axial direction. This was confirmed by viewing the Pronto3D results, which indicated an essential planar motion of the shell mesh over time.

There remains the question of the over-predicted plate velocities with Zapotec. Comparison of the CTH-3D and Zapotec calculations run at the same mesh resolution can provide some insight into the differences. Tracers were embedded in the explosive along the problem centerline at z-coordinate locations of 5, 10, and 15 mm. Pressure and impulse histories compared well between the two calculations (a maximum of 0.8 and 2.9 percent difference in specific impulse noted at the 15 mm station for the fine and coarse-meshed calculations, respectively), suggesting that the inserted material state did not significantly affect the CTH portion of the analysis. There were, however, noticeable differences in the total internal energy for the plate material, with the Zapotec inserted material staying essentially at the reference state. It is conjectured that the shell-mesh behaved as a rigid body and no work was done on the material. Consequently, the plate accelerated faster in the Zapotec calculation, resulting in a higher asymptotic plate velocity. It is not clear if this effect becomes amplified as the CTH mesh is coarsened, since the detonation process itself is affected by the CTH mesh resolution.

As an aside, a series of excursion calculations were conducted to assess the influence of scale factor applied to the effective shell thickness. The results are also provided in Table 1. As the scale factor is increased, the expanded shell covers more CTH cells along the top direction. The choice of scale factor does not significantly affect the calculated velocity, at least for this particular application and choice of mesh resolution.

AIR BLAST ON A THIN FLAT PLATE

Boyd [9] conducted a series of experiments to investigate the response of thin, flat steel plates subjected to a blast loading. These experiments involved suspending a 250-g spherical pentolite charge in air over a square plate at various charge standoffs. The underlying square plate was 5-mm-thick, with a width of 1.2 m and was bolted to a heavy steel frame. The steel frame was set in groves within underlying support blocks. After placement, the plate had a 1.0 m square area free to displace under load. Pressure gauges and accelerometers were placed along the plate diagonals 0.1 and 0.2 m from its center. A displacement gauge was also positioned under the center of the plate. Test E17 will be modeled with Zapotec. The charge standoff was 0.25 m.

Taking advantage of the symmetry of the experimental setup, it was possible to model only a quarter of the problem. The initial problem geometry is illustrated in Fig. 7. The problem is composed of four materials: the explosive charge, plate, support blocks, and surrounding air. The charge and air were modeled as Eulerian materials, while the plate and support blocks were modeled as Lagrangian materials.

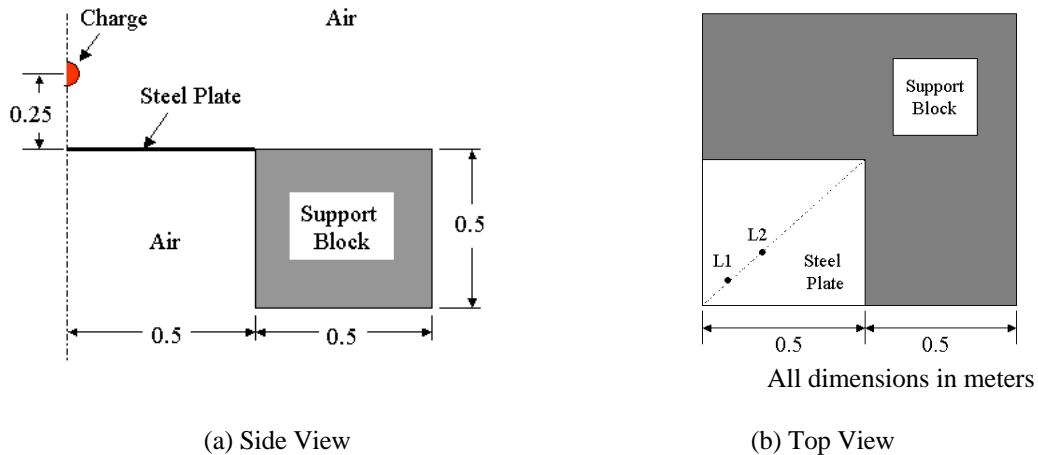


Figure 7. Initial Problem Geometry

The CTH mesh encompassed the charge, plate, and support blocks. Air was inserted throughout the entire Eulerian domain such that it surrounded all solid bodies in the problem. A uniform mesh was assumed in the region encompassing the steel plate. The mesh was graded laterally over the support block with a 10 percent grading factor. Two cell widths in the uniform region were considered for the parameter study, 5 and 20 mm. Extrapolated pressure boundary conditions were applied to the outer bounds of the CTH mesh. The CTH material library JWL EOS for pentolite was used for the explosive charge, with a programmed burn option and detonation at the charge center assumed. The CTH library SESAME EOS was used for the air. Both materials were modeled as hydrodynamic.

The Lagrangian steel plate was modeled as an elastic-plastic material based on properties supplied in [9] ($\rho = 7.85$ g/cc, $E = 103.1$ GPa, $\nu = 0.30$, $\sigma_o = 270$ MPa, $E_T = 470$ MPa). The plate was modeled using a uniform mesh of Key-Hoff shell elements having a thickness and width of 5 and 10 mm, respectively. The solid support block was assumed to be composed of steel material, which effectively created a rigid support structure. The support block was discretized using 8-node hexahedral elements. The nodes at the joint formed between the plate and support were collocated, with clamped boundary conditions assumed at the joint. These boundary conditions differ from that in the actual experimental setup, which involved bolting the plate to a heavy steel frame. The base of the support was fixed to prevent any translation. Nodal history data were also obtained (at the plate center and along its diagonals, 0.1 and 0.2 m from the center) for comparison with the experimental results.

As with the previous example, different expansion distances were chosen for the top and bottom surfaces of the shell mesh. Shells were expanded along the top direction (i.e., on the side impinged by the blast wave) to half of the plate thickness so that their expanded thickness coincided with the plate's true surface location. Opposite this interface, shell elements were expanded to cover at least two CTH cells into the adjacent air space (i.e., scale = 2.0 in Eq. (1)). Loads generated by the blast were applied along the top surface of the expanded shell elements and support block.

For this problem, the duration of the blast loading is expected to be much less than the response time of the structure. To reduce the computational expense, the coupled analysis was run for 0.6 msec, after which the CTH portion of the analysis was turned off and the Pronto3D calculation was allowed to continue to 300 msec. This was more than sufficient to capture the permanent deflection of the plate. Review of the load history on the plate indicated the blast loading phase was over by 0.6 msec.

Comparisons with the experimental results are provided in Table 2. Comparisons are drawn with the peak accelerations at both accelerometer locations (denoted L1 and L2), the peak displacement at the plate center, and the permanent displacement at the center. Locations L1 and L2 coincide with the locations along the plate diagonals of 0.1 and 0.2 m from center. One notes a significant increase in the calculated accelerations with mesh refinement, and only a marginal increase in the displacements. The calculated acceleration correlates directly with the strength of the shock wave impinging on the plate. As the mesh is refined, the peak pressures increase at the shock front and pressure gradients are better resolved. In contrast, the displacement results vary as a weak function of the mesh resolution. This is not surprising, as this measurement correlates more with the impulse delivered to the plate, which is less dependent on mesh resolution. Comparison of the displacement results indicates the peak centerline velocities are severely under-predicted; however, good comparisons are noted for the permanent displacement.

Table 2. Comparison with Experimental Results

CTH Cell Width (cm)	Acceleration (g)		Peak Centerline Displacement (mm)	Permanent Centerline Displacement (mm)
	Location L1	Location L2		
Experiment	40,969	30,049	35	9
2.0	24,159	19,062	24	10
0.5	63,201	32,299	25	13

BLAST LOADING INDUCED FROM A BURIED LAND MINE

The final example models the response of a flat plate subjected to a mine blast. The problem setup is based on a calculation done by Lottero and Kimsey [10]. Their calculation involved a one-way coupled analysis with the blast loading on a rigid surface computed using the Eulerian hydrocode DORF, which was subsequently applied as a pressure patch input to the structural analysis code REPSIL (see [10] for details). The problem geometry, as modeled by Zapotec, is illustrated in Fig. 8. The land mine is modeled as a cylindrical 0.265-kg C-4 charge, which is buried 57 mm from the surface. A 6.78-mm-thick, 254-mm-square rolled-homogeneous armor (RHA) plate is set within a mounting bracket, allowing for an 89 mm gap of air between it and the underlying soil. The plate is set into the mounting bracket such that clamped conditions exist at the joint between the plate and mount. The geometry for the mounting bracket was assumed, since no details were provided in [10]. The 193 mm width of the mount was chosen to match the mesh width used in the original DORF calculation.

For the Zapotec analysis, the explosive, soil, and air were modeled as Eulerian materials, while the RHA plate and mount were modeled as Lagrangian. A uniform CTH mesh having a cell size of 0.5 mm was assumed in the interaction region encompassing the plate, which enclosed a region going from the centerline out to a lateral distance of 200 mm. From there, the mesh was graded along the lateral directions. Transmissive boundary conditions were applied to the lateral extents of the CTH mesh. The explosive and air were modeled as hydrodynamic materials using the CTH material library JWL EOS for C-4 and the SESAME EOS for air. A program burn was assumed with the detonation point specified at the charge base. The soil was described as a dry tuff in [10], with material data specified for a Tillotson EOS. No description of the deviatoric response was provided. For the Zapotec analysis, the soil was assumed to resemble Sidewinder Tuff, which has been previously characterized using a P-alpha EOS and geologic strength model in CTH (see [1] for material parameters and description of model fits). The assumed soil type represents a very weak assumption, made necessary due to a lack of detailed soil characteristics data and lack of support for the Tillotson EOS in CTH.

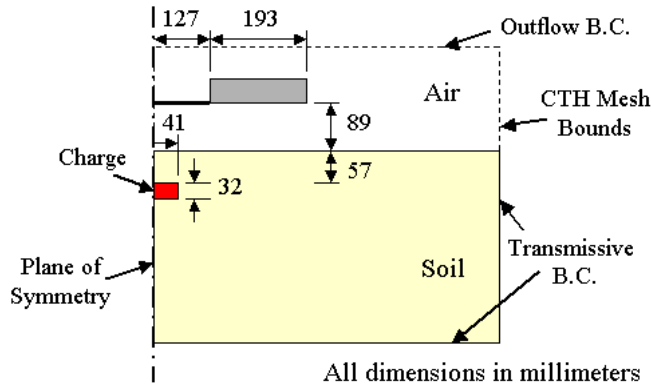


Figure 8. Zapotec Problem Setup

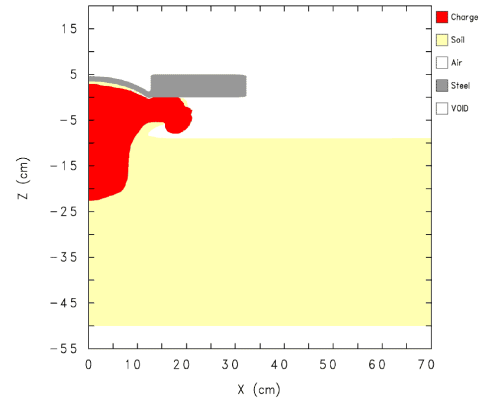


Figure 9. Material Plot at 0.6 msec

The RHA plate and mounting bracket (assumed as steel) were modeled with the Johnson-Cook constitutive model using material data for 4340 steel as described in [8]. The plate was modeled using a uniform mesh of Key-Hoff shell elements having a specified thickness and width of 6.78 and 6.35 mm, respectively. The mounting bracket was meshed using 8-node hexahedral elements. The nodes at the joint formed between the plate and mounting bracket were collocated, with clamped boundary conditions assumed at the joint.

For the Zapotec analysis, shell elements were expanded along the bottom direction (i.e., on the side impinged by the blast and soil ejecta) to half of the plate thickness so that their expanded thickness coincided with the plate's true surface location. Shell elements were expanded along the top direction with an assumed scale factor of 2.0 applied to the effective shell thickness. Loads were applied only to the bottom surface of the plate and mounting bracket, which was impinged by either the blast products or soil ejecta.

The detonation results in the near-instantaneous formation of a soil cavity filled with expanding gaseous products in a state of high pressure and temperature. The expanding gases impart a high radial velocity to the surrounding soil, with an accompanying compressive wave transmitted into the soil. In this example, the detonation occurs relatively near the soil surface, resulting in explosive gases venting into the air and the formation of a crater as soil ejecta is thrown outwards. By 25 μsec , the compressive wave has reached the soil/air interface. The incident compressive wave reflects off the free surface, resulting in a relief wave transmitted back into the soil with subsequent motion of soil upwards into the air space. Further bulging of the soil occurs over time as the incident wave moves radially outward from the detonation centerline and interacts with the free surface. At approximately 200 μsec , a mixture of explosive products and soil ejecta reaches the plate. Over time, the continued loading of blast products and ejecta results in plate deformation as illustrated in Figure 9. The DORF calculation in [10] indicates the soil first reaches the plate at 112 μsec . The disparity in the timings can likely be attributed to differences in modeling the soil.

Lottero and Kimsey predicted a maximum plate deflection of 55.9 mm with no tearing. This compared well with an empirical model also discussed in [10], which predicted a maximum deflection of 51.3 mm. In contrast, Zapotec predicted a maximum deflection of 39.4 mm, which is approximately 23 percent below that predicted by the empirical model. Disparities associated with modeling the soil can account for some of the difference. For example, there are known differences for the initial dry density and water content for the two soils (1700 kg/m^3 and 5 percent moisture for the tuff described in [10] versus 1800 kg/m^3 and 2 percent moisture for the Sidewinder Tuff). However, it is unclear that soil modeling alone can account for the large under-prediction of the plate deflection. Further parametric studies are needed to assess the sensitivity of the analysis to material modeling as well as the optional inputs associated with the shell reconstruction algorithm. Regardless, this example provides some demonstration of Zapotec's ability to model this class of problem.

CONCLUDING REMARKS

The shell reconstruction algorithm is a new capability implemented into Zapotec. Further investigation of the algorithm and its application is needed. Future work will address modeling issues associated with the algorithm, which include: (1) assessing differing mesh resolutions on the Eulerian and Lagrangian domains, and its subsequent effect on the loading applied to a Lagrangian body, (2) additional testing to assess the effect of expansion thickness on the CTH calculation, (3) mapping of the stress based on an average state over all integration points, and (4) modeling of complex thin-shell structures (e.g., T-sections, box-frame structures, etc.).

ACKNOWLEDGEMENTS

Special thanks to Marlin Kipp (SNL) who assisted with development of the validation problems for the shell reconstruction algorithm. Sandia is a multi-program laboratory operated by Sandia Corporation, a Lockheed Martin Company, for the United States Department of Energy under Contract DE-AC04-94AL85000.

REFERENCES

- [1] Bessette, G.C., Vaughan, C.T., and Bell, R.L., "Zapotec: A Coupled Euler-Lagrange Program for Modeling Earth Penetration", *Proc. 73rd Shock and Vibration Symposium*, 2002 (in-publication).
- [2] Bessette, G., Vaughan, C., Bell, R., and Attaway, S., 2003, "Zapotec: A Coupled Methodology for Modeling Penetration Problems", *Fluid Structure Interaction II*, Wessex Institute of Technology Press, pp. 273-282.
- [3] McGlaun, J.M., Thompson, S.L., and Elrick, M.G., "CTH: A Three-Dimensional Shock Wave Physics Code", *Int. J. of Impact Engineering*, 1990, Vol. 10, pp. 351-360.
- [4] Hertel, E.S., Bell, R.L., Elrick, M.G., Farnsworth, A.V., Kerley, G.I., McGlaun, J.M., Petney, S.V., Silling, S.A., Taylor, P.A., and Yarrington, L., 1993, "CTH: A Software Family for Multi-Dimensional Shock Physics Analysis", Sandia National Laboratories Report SAND92-2089C.
- [5] Taylor, L.M., and Flanagan, D.P., 1989, "Pronto3D, A Three-Dimensional Transient Solid Dynamics Program", Sandia National Laboratories Report SAND87-1912.
- [6] Attaway, S.W., Mello, F.J., Heinstein, M.W., Swegle, J.W., Ratner, J.A., and Zadoks, R.I., 1998, "Pronto3D Users' Instructions: A Transient Dynamic Code for Nonlinear Structural Analysis", Sandia National Laboratories Report SAND98-1361.
- [7] Lee, E., Breithaupt, D., McMillan, C., Parker, N., Kury, J., Tarver, C., Quirk, W., and Walton, J., "The Motion of Thin Metal Walls and the Equation of State of Detonation Products", *Proc. Eight Symposium (International) on Detonation*, 1985, pp. 613-624.
- [8] Johnson, G.R., and Cook, W.H., "Fracture Characteristics of Three Metals Subjected to Various Strains, Strain Rates, Temperatures, and Pressures", *Engineering Fracture Mechanics*, 1985, Vol. 21, pp. 31-48.
- [9] Boyd, S.D., 2000, "Acceleration of a Plate Subject to Explosive Loading – Trial Results", Dept. of Defense, Defense Science and Technology Organization, Aeronautical and Maritime Research Laboratory, Melbourne, Australia Report DSTO-TN-0270.
- [10] Lottero, R.E., and Kimsey, K.D., 1978, "A Comparison of Computed Versus Experimental Loading and Response of a Flat Plate Subjected to Mine Blast", USA Ballistic Research Laboratories Report ARBRL-MR-02807.